J Fluoresc (2015) 25:973–978
DOI 10.1007/s10895-015-1578-1

ORIGINAL PAPER

Fluorescence Quenching of Perylene DBPI Dye by Colloidal Low-Dimensional Gold Nanoparticles

Samy A. El-Daly[1,3] · **Mohammed M. Rahman**[1,2] · **Kalid A. Alamry**[1] · **Abdullah M. Asiri**[1,2]

Received: 10 February 2015 / Accepted: 4 May 2015 / Published online: 16 May 2015

Abstract The interaction of a perylene DBPI dye [*N,N*-bis(2,5-di-tert-butylphenyl)-3,4:9,10-perylenebis(dicarboximide)] with aqueous colloidal gold nanoparticles (AuNPs) was studied using steady state fluorescence quenching measurements. The Stern–Volmer quenching rate constant (K_{sv}) was calculated as ~2.2×10^8 and ~1.072×10^9 M^{-1} in ethanol and ethylene glycol respectively. From fluorescence quenching data, the static quenching and energy transfer play a significant role in the fluorescence quenching of DBPI with AuNPs. The apparent association constant (K_{app}) was calculated as ~1.4×10^9 (EtOH)and ~3.7×10^9 M^{-1} (ethylene). Due to AuNPs interaction with DBPI, the average aggregated colloidal AuNPs size is increased from ~53.39 nm (before interaction) to ~94.12 nm (after interaction).

Keywords Colloidal gold nanoparticles · Perylene DBPI · Fluorescence · Quenching · Stern–volmer interaction

Introduction

N, N-Bis(2,5-di-tert-butylphenyl)-3,4:9,10-perylenebis(dicarboximide) (DBPI) is potentially useful in energy and electron transfer reactions [1, 2], site-selective spectroscopy experiments with biological systems [3, 4], solar cells [5], and as a laser dye [6]. Various photophysical characteristics of DBPI have been studied, including fluorescence quenching, excitation energy transfer [7–10], fluorescence quantum yield and high-photostability [11], amplified spontaneous emission and electrochemical properties [12]. The effect of morphologically-dependent resonances on the fluorescence of DBPI dissolved in polymer microparticles and microcrystals has also been reported [13, 14]. Diffraction efficiency of laser-induced transient gating and relaxation time of DBPI has been studied [15]. The molecular structure of DBPI is presented in Fig. 1.

Potential application of nano-scale material and molecular structures ranging from 1.0 to 100.0 nm is a promising area of nano-science and nano-technology. Metallic nanoparticles have large and highly specific surface areas with a prominent fraction of surface atoms and have been investigated because of their unique physico-chemical properties including photo-catalytic activity, optical or electronic sensors, anti-bacterial activity, and magnetism [16–20]. On-site preparation of noble nanoparticles for the potential applications such as photo-catalysis, opto-electronics, environmental, electrochemical, and biotechnology is an area of growing attention [21, 22]. Usually, metallic low-dimensional nanoparticles are prepared and stabilized by chemical techniques such as chemical reduction, electro-chemical, photo-chemical reactions, controlled thermometric, and recently by green chemistry methods [23–27]. Use of reducing agents with surfactants in synthesis and quenching of metallic nanoparticles with anchoric dye offers an improvement over physico-chemical techniques since it is economic, environmentally acceptable and easily scaled up for large scale preparation. Using this technique, there is no need

✉ Mohammed M. Rahman
mmrahman@kau.edu.sa

[1] Chemistry Department, Faculty of Science, King Abdulaziz University, P.O. Box 80203, Jeddah 21589, Saudi Arabia

[2] Center of Excellence for Advanced Materials Research (CEAMR), King Abdulaziz University, Jeddah 21589, P.O. Box 80203, Saudi Arabia

[3] Chemistry Department, Faculty of Science, Tanta University, Tanta, Egypt

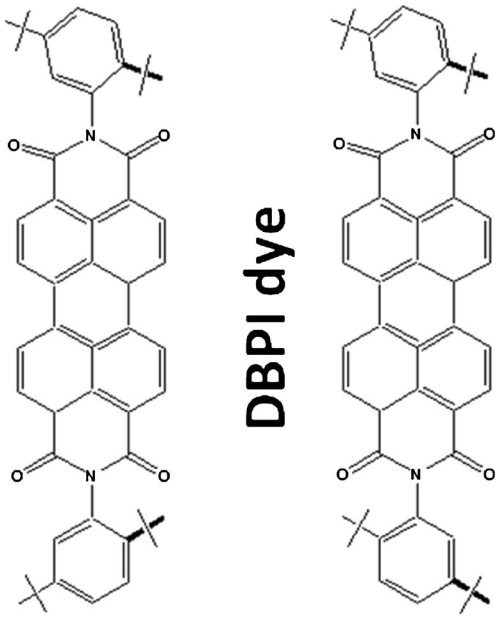

Fig. 1 Molecular structure of DBPI dye

to use high pressure, high temperature, sophisticated tools or expensive and toxic chemicals. DBPI is an important highly photostable probe molecule. To the best of our knowledege, there is no any report on fluorescence quenching of DBPI by gold nanoparticles. In the present work, we studied the fluorescence quenching by low-dimensional gold nanoparticles in ethanol and ethylene glycol in order to determine the mechanism of energy transfer from DBPI to gold nanoparticles.

Experimental

Chloroform, methanol, ethanol, chloroform, ethylene glycol, $AuCl_3$, tri-sodium citrate, and $NaBH_4$ were purchased from Sigma-Aldrich and used as received without any further treatments. All solvents used in this experiment were of spectroscopic grade. DBPI (Aldrich) was dissolved in a minimum volume of chloroform. The DBPI dye was precipited by adding methanol solvent. The precipitate was collected by filtration and dried in vacuum. Low-dimensional gold nanoparticles (AuNPs) were prepared by a chemical reduction route with tri-sodium citrate as surfactant. In a typical synthetic procedure, 50.0 ml of 0.01 M gold chloride ($AuCl_3$) was stirred with 0.1 M trisodium citrate at room temperature for 10.0 min. To this mixture, 50.0 ml of 0.1 M of ice-cold reducing agent ($NaBH_4$) was added drop-wise and the resulting mixture was stirred for 20 min. After about 20 min, the original transparent solution of $AuCl_3$ and tri-sodium citrate turned light-yellow color indicating the formation of aggregated gold nanoparticles. Steady state emission spectra were measured with a Shimadzu RF 5300 spectro-fluorometer using a rectangular quartz cell (dimensions 0.2×1.0 cm) to minimize reabsorption effect. UV-visible electronic absorption spectra were measured using a Shimadzu UV-visible 1650-pc spectrophotometer. Morphology, size, and structure of gold nanoparticles were recorded on FESEM instrument (JSM-7600F, Japan).

AuCl3, tri-sodium citrate, and NaBH4

Results and Discussion

Steady State Emission Measurements

Figure 2 shows the fluorescence spectra of 1.0×10^{-6} mol dm^{-3} of DBPI in the presence of variable concentrations

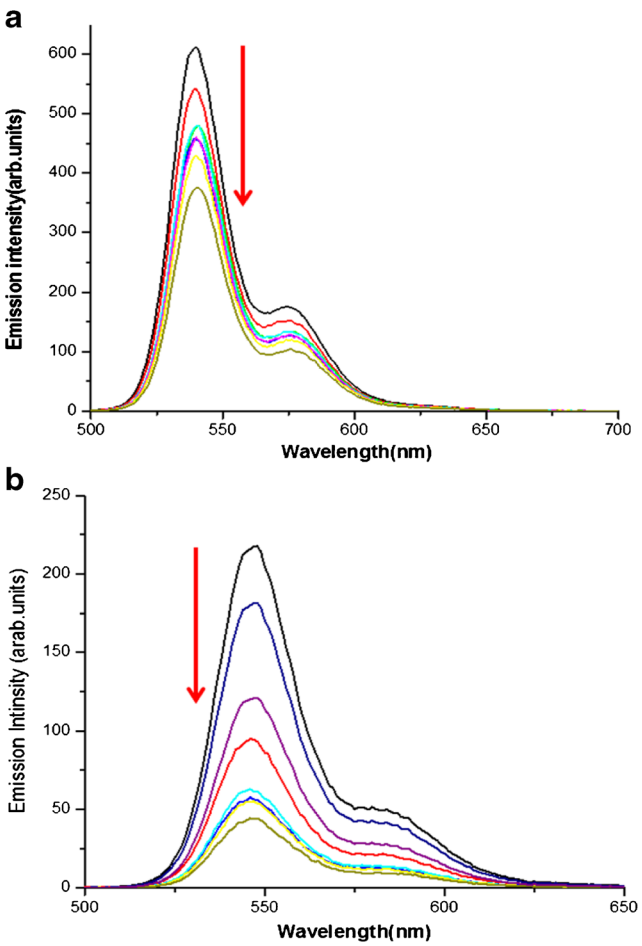

Fig. 2 **a** Emission spectra of 1.0×10^{-6} mol dm^{-3} solution of DBPI in EtOH in presence of different concentrations of AuNPs . The concentrations of AuNPs at decreasing emission intensity are 0.0, 0.277, 0.555, 1.109, 1.387, 1.664,1.942 and 2.219 nM (λ_{ex}=480.0 nm); **b** Emission spectra of 1.0×10^{-6} mol dm^{-3} solution of DBPI in ethylene glycol in the presence of different concentrations of AuNPs . The concentrations of AuNPs at decreasing emission intensity are 0.0, 0.138, 0.277, 0.555, 1.1096, 1.387, $\frac{I_o}{I} = 1 + K_{SV}$ [Au] 1.664, 1.942, and 2.19 nM (λ_{ex}=480.0 nm)

of gold nanoparticles in ethanol and ethylene glycol. The fluorescence emission of DBPI exhibits a maximum at ~548.0 nm upon excitation at ~480.0 nm. As the concentration of quencher was increased, λ_{max} of the fluorescence bands of DBPI did not change but a substantial decrease in fluorescence intensity was observed. This indicates the absence of molecular aggregation under the prevailing experimental conditions. Under the experimental conditions used, the excitation wavelength of ~480.0 nm was about 80.0 nm from the maximum of absorption peak of gold nanoparticles; no such quenching of DBPI was seen in the presence of the low concentrations of capping agent indicating that gold nanoparticles are responsible for the fluorescence quenching.

Figure 3 shows the Stern–Volmer plot derived from Eq (1) of DBPI fluorescence quenching using gold nanoparticles as a quencher [28]

$$\frac{I_o}{I} = 1 + K_{SV}[Au] \quad (1)$$

where Io and I are the fluorescence intensities in the absence and presence of the quencher concentration [Au^o].

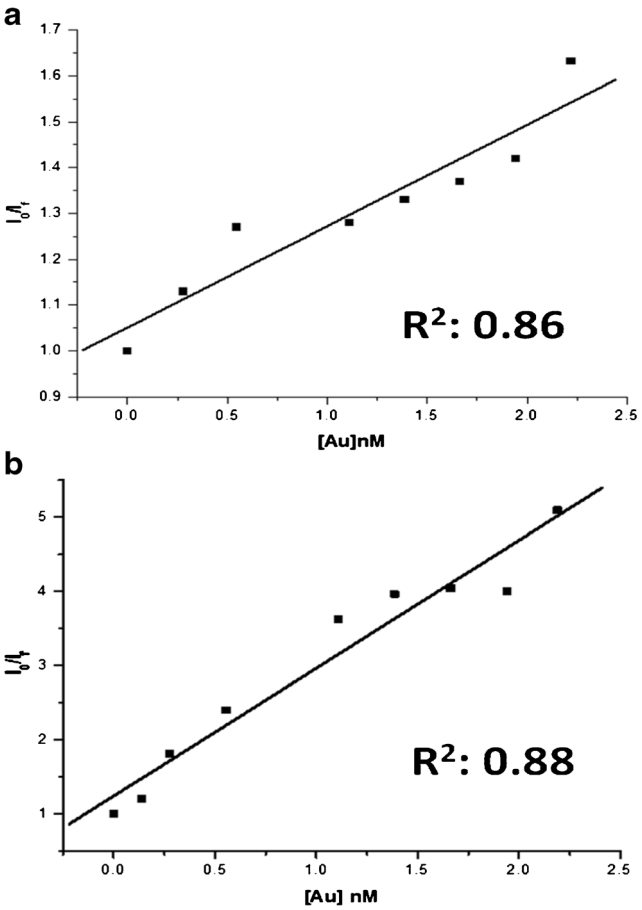

Fig. 3 Stern–Volmer plot of fluorescence quenching of DBPI by AuNPs. **a** in ethanol and **b** in ethylene glycol

The was calculated as 2.2×10^8 and 1.07×10^9 M^{-1} in ethanol and ethylene glycol respectively. The quenching efficiency increases as the medium viscosity increases indicating that the quenching process is not completely diffusion–controlled. This is consistent with a static quenching model in which increasing the medium viscosity leads to a cage effect that enhances fluorophore uptake on gold nanoparticles surfaces. Taking the fluorescence lifetime of DBPI in absence of gold nanoparticles as 3.5 ns [8], the values of the bimolecular quenching rate constant (k_q)=K_{sv} /τ are calculated as 6.2×10^{16} and 3.11×10^{17} M^{-1} s^{-1} in ethanol and ethylene glycol respectively. These values are much higher than the diffusion rate constant k_d (k_d=9.2×10^{10} M^{-1} for ethanol and 5.8×10^8 M^{-1} for ethylene glycol). It is concluded that static quenching and Forster-type energy-transfer plays a major role in fluorescence quenching beween DBPI and AuNPs, due to a significant overlap between electronic absorption of AuNPs and emission of DBPI. In addition, the reverse effect of ethylene glycol on K_{sv} values indicates that static quenching plays a major role in the quenching of DBPI by gold nanoparticles.

The Perrin-model is valid for energy transfer between donor–acceptor components unable to change spatial position with respect to each other on the time scale of the quenching process. The Perrin relationship [29, 30] is given by Eq. (2):

$$\ln\left(\frac{I_o}{I}\right) = VN_o[Q] \qquad V = \frac{4}{3}\pi r^3 \quad (2)$$

where I_o and I are emission intensities in the absence and presence of quencher, V is the volume of the quenching sphere in cubic centimeters, N_o is the Avogdaro's number, [Q] is the molar concentration of the quencher, and r is the radius of quenching sphere volume. A plot of ln $\left(\frac{I_o}{I}\right)$ versus [Q] (Fig. 4) should demonstrate linear behavior with slope equal to VN_o . V values were found to be 2.82×10^{-16} (r=40.6 nm) and 1.11×10^{-15} cm^3 (r=64.2 nm) in ethanol and ethylene glycol, respectively.

We can express the equilibrium between adsorbed and unadsorbed DBPI dye molecules by Eq. (4). Here, k_{app} is the apparent association constant which can be calculated from the fluorescence data according to Eq. (4) [31] (Fig. 5),

$$\text{DBPI} + \text{Au} \leftrightarrow [\text{DBPI}\cdots\text{Au}] \quad (3)$$

$$k_{app} = [DBPI\cdots\cdots Au] \,/\, [DBPI]\,[Au] \quad (4)$$

$$\frac{1}{F^o - F} = \frac{1}{F^o - F'} + \frac{1}{K_{app}} \times \frac{1}{F^o - F'} \times \frac{1}{Au} \quad (5)$$

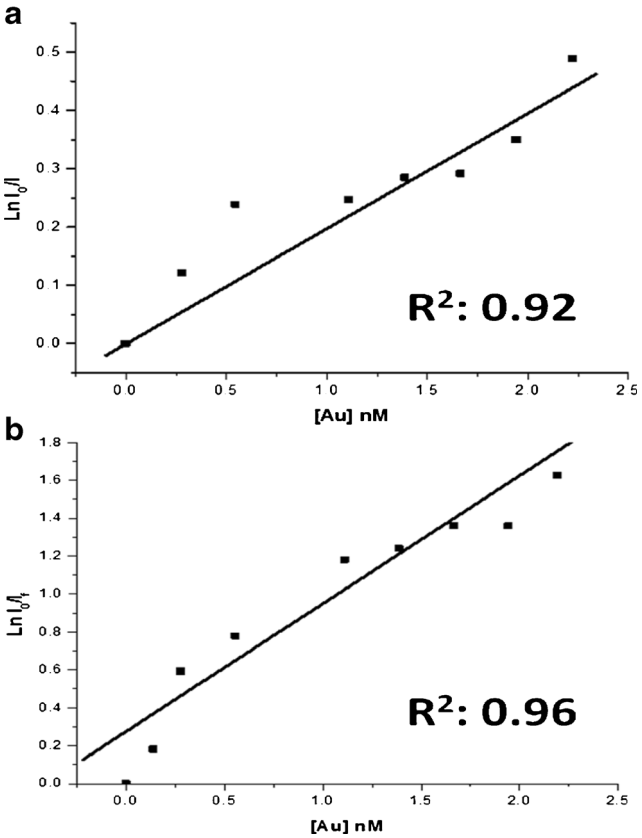

Fig. 4 Perrin-plot of fluorescence quenching of DBPI by Au NPs. **a** in ethanol and **b** in ethylene glycol

where F^o, is the initial fluorescence intensity of dye molecules, F′ is the fluorescence intensity of Au adsorbed dye and F is the observed fluorescence intensity at its maximum. The physical interaction between DPBI molecules and AuNPs is investigated using Benesi–Hildebrand approach by Eq. 5. The calculated k_{app} values are 1.4×10^9 and 3.7×10^9 M^{-1} for ethanol and ethylene glycol, respectively which indicate the viscosity of the medium play an important role for interaction of DPBI molecules with AuNPs.

Investigation of AuNPs Interaction with DBPI Dye

UV/visible spectroscopy referred to absorption spectroscopy in the UV-Visible spectral region. Absorption in the visible range directly affects the apparent color of the target materials involved in this region of the electromagnetic spectrum, where the target molecules undergo electronic transitions. The formation of metallic gold nanoparticles (eg, AuNPs) by $NaBH_4$ reduction of the aqueous metal ions in presence of surfactant (tri-sodium citrates) is investigated using UV/vis. Spectroscopy, which is presented in Fig. 6a. Fluorescence quenching is exhibited by the downfall of arrow, which indicated the emission intensity is decreased significantly by the interaction of DBPI-AuNPs (Fig. 6b). The wavelength of prepared AuNPs solution remains close to ~431.0 nm in the aqueous system, suggesting that the NPs were well-dispersed in the aqueous medium. The probable interaction of a DBPI-dye molecule with AuNPs is presented schematically in Fig. 6c.

FESEM is a method whereby a beam of electrons is transmitted through an ultra-thin specimen, interacting with the sample as it passes through. An image is generally formed from the interaction of the electrons transmitted through the specimen; the image is magnified and focused onto an imaging target. FESEM analysis exhibited that the AuNPs prepared by this technique had an average size of ~53.39±5.0 nm (ranges, 45.0 to 60.0 nm), which is presented in Fig. 6d. It is concluded that the prepared nanoparticles are spherical in morphology and stable. Finally the AuNPs are stabilized by

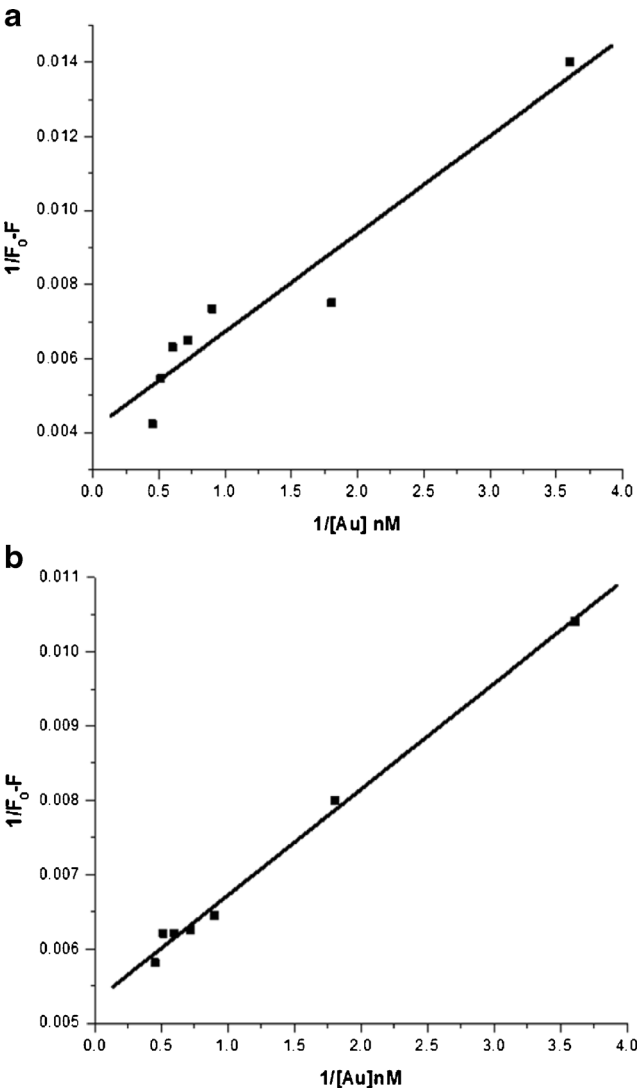

Fig. 5 Benesi–Hildebrand plot for the adsorption of DBPI on Au NPs: **a** in ethanol and **b** in ethylene glycol

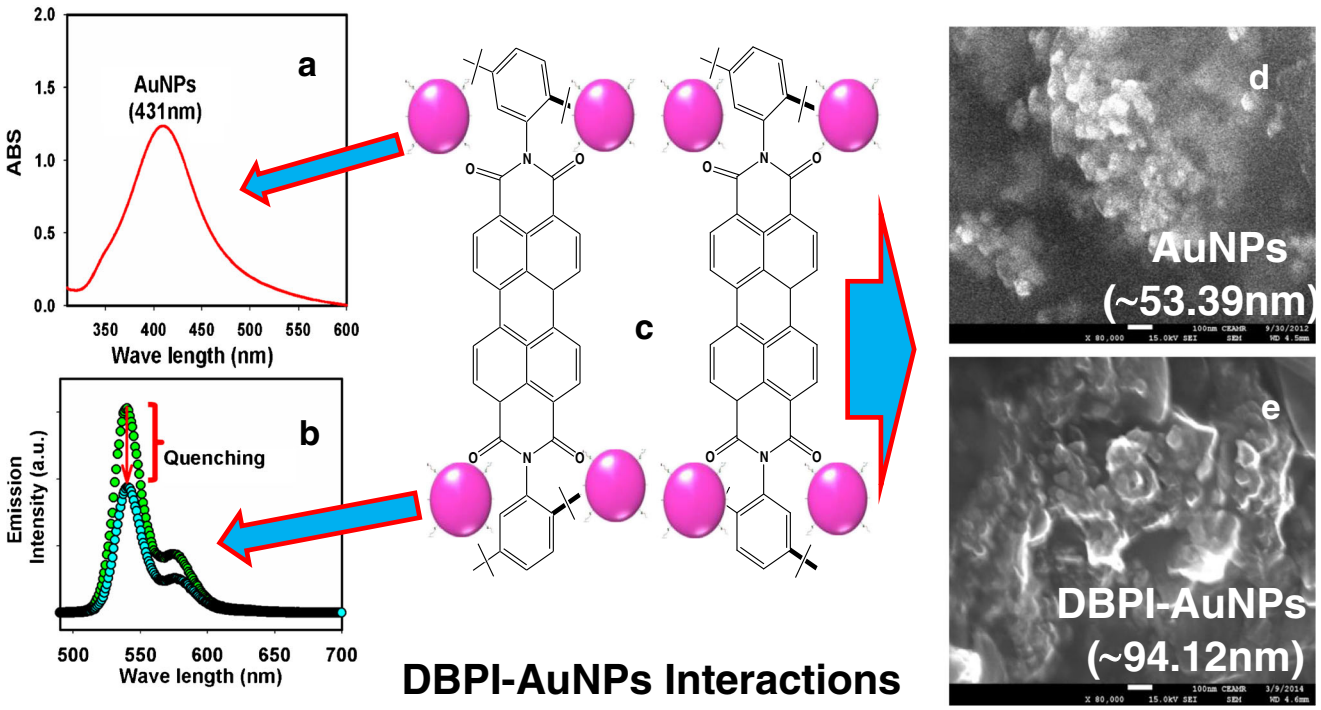

Fig. 6 A schematic representation of the formation of DBPI dye-AuNPs interactions. **a** UV/visible spectrum of AuNPs prepared by reducing agent in presence of active surfactants (λ_{max}=431.0 nm), **b** Fluorescence quenching is shown by the *arrow* (Emission intensity is decreased by the interaction of DBPI-AuNPs), **c** Interaction of AuNPs-DBPI, **d** FESEM image of AuNPs, and **e** FESEM image of DBPI adsorbed AuNPs

aggregation of adsorbed citrate ions with the corresponding cation around them.

This DBPI-molecule has four carbonyl groups, which it can be bonded with AuNPs. Thus, it is more electronegative and can bind to NPs significantly to form a DBPI-AuNPs complex. Due to the affinity of DBPI-dye molecule with AuNPs, electron transfer becomes easier as is demonstrated from earlier fluorescence investigation. Due to potential AuNPs interaction with DBPI dye, the average AuNPs size is increased from ~53.39 nm (before interaction) to ~94.12 nm (after interaction). The diameter of DBPI dye interacted AuNPs is enlarged by ~40.73 nm, which is presented in Fig. 6d–e.

Conclusions

DBPI displays fluorescence quenching by colloidal AuNPs in ethanol and ethylene glycol simultaneously. From quenching data, static quenching and energy transfer from excited dye to AuNPs play a significant role in the quenching in fluorescence of DBPI by AuNPs. The Stern–Volmer quenching rate constant (K_{sv}) was calculated as ~2.2×10^{8} and ~1.072×10^{9} M^{-1} in ethanol and ethylene glycol respectively. The apparent association constant (K_{app}) was calculated as ~1.4×10^{9} (EtOH) and ~3.7×10^{9} M^{-1} (ethylene). Due to AuNPs interaction with DBPI, the average aggregated colloidal AuNPs size is increased from ~53.39 nm (before interaction) to ~94.12 nm (after interaction).

References

1. Balzani V, Bolletta F, Scandola F, Ballardini R (1965) Excited state electron-transfer reactions of transition metal complexes. Pure Appl Chem 51:299–311
2. Darwent JR, Douglas P, Harriman A, Rickoux GMC (1982) Metal phthalocyanines and porphyrins as photosensitizers for reduction of water to hydrogen. Coord Chem Rev 44:83–126
3. Kavarnos GJ, Turro NJ (1986) Photosensitization by reversible electron transfer. Chem Rev 86:401–449
4. El-Daly SA, Asiri AM, Alamry KA (2014) Experimental determination of ground and excited state dipole moments of N, N-Bis (2, 5-di-tert-butylphenyl)-3, 4:9, 10-perylenebis (dicarboximide) (DBPI) a photostable laser dye. J Fluoresc 24:1307–1311
5. Sandra M, Bird GR (1984) Semiconductor laser amplifier for single mode optical fiber communications. Opt Commun 51:62
6. Ford WE, Kamat PV (1987) Photochemistry of 3,4,9,10-perylenetetracarboxylic dianhydride dyes. 3. Singlet and triplet excited-state properties of the bis(2,5-di-tert-butylphenyl)imide derivative. J Phys Chem 91:6373
7. El-Daly SA (1992) Fluorescence quenching of N, N-bis(2,5-di-tert-butylphenyl)-3,4:9,10-perylenebis(dicarboximide) (DBPI) by Co2+ ion. J Photochem Photobiol A Chem 68:51–58
8. El-Daly SA, Okamoto M, Hirayama S (1995) Fluorescence quenching of N, N'-bis(2,5-di-tert-butylphenyl)-3,4:9,10-

perylenebis(dicarboximide) (DBPI) by molecular oxygen. J Photochem Photobiol A Chem 91:105–110
9. El-Daly SA, Hirayama S (1997) Re-absorption and excitation energy transfer of N, N'-bis(2,5-di-tert-butylphenyl)-3,4:9,10-perylenebis(dicarboximide) (DBPI) laser dye. J Photochem Photobiol A Chem 110:59–65
10. El-Kemary MA, El-Daly SA (1996) Interaction of the excited singlet state of 1,4- and 1,8-dimethoxynaphthalene with some organic compounds: a fluorescence-quenching study. Monatsh Chem 127:593–600
11. Ebeid EM, El-Daly SA, Langhals H (1988) Emission characteristics and photostability of N, N'-bis(2,5-di-tertbutylphenyl)-3,4:9,10-perylenebis (dicarboximide). J Phys Chem 92:4565–4568
12. El-Hallag IS, El-Daly SA (2010) Photophysical and electrochmical studies of N, N-Bis (2,5-di-tert-butylphenyl) -3,4,9,10 perylenebis (dicarboximide) (DBPI). Bull Kor Chem Soc 31:989–998
13. Bisht PB, Fukuda K, Hirayama S (1996) Normal mode theory of two step relaxation in liquids: polarizability dynamics in CS2. J Chem Phys 105:9349–9356
14. Bisht PB, Fukuda K, Hirayama S (1997) Steady-state and time-resolved fluorescence study of some dyes in polymer molecules embedded in spherical dielectric particles. J Phys Chem B 101: 8054–8085
15. Justin RJ, Bish PB (2000) Theoretical and experimental studies on photophysical parameters of N, N'-bis(2,5,-di-tert-butylphenyl)-3, 4:9-10-perylenebis(dicarboximide) (DBPI) by using transient grating technique. Chem Phys Lett 357:420–425
16. Saxena A, Tripathi RM, Singh RP (2010) Biological synthesis of silver nanoparticles by using onion (Allium cepa) extract and their antibacterial activity. Digest J Nanomater Biostruc 5:427–432
17. Catauro M, Raucci MG, De-Gaaetano FD, Marotta A (2004) Antibacterial and bioactive silver containing $Na_2O.CaO{\times}2SiO_2$ glass prepared by sol–gel method. J Mater Sci Mater Med 15: 831–837
18. Crabtree JH, Brruchette RJ, Siddiqi R, Huen I, Handott LL, Fishman A (2003) The efficacy of silver-ion implanted catheters in reducing peritoneal dialysis-related infections. Perit Dial Int 23:368–374
19. Krolikowska A, Kudelski A, Michota A, Bukowska (2003) SERS studies on the structure of thioglycolic acid monolayers on silver and gold. J Surf Sci 532:227–232
20. Zhao G, Stevens JS (1998) Multiple parameters for the comprehensive evaluation of the susceptibility of escherichia coli to the silver ion. Biometals 11:27–32
21. Hussain I, Brust M, Papworth AJ, Cooper AI (2003) Extracellular biosynthesis of monodisperse gold nanoparticles by a novel extremophilic actinomycete, *Thermomonospora* sp. Langmuir 19: 3550–3553
22. Virender KS, Ria AY, Yekaterina L (2009) Silver nanoparticles: green synthesis and their antimicrobial activities. Colloid Interface Sci 145:83–96
23. Krishna B, Goia DV (2009) Silver nanoparticles for printable electronics and biological applications. J Mater Res 24:2828–2836
24. Tripathi RM, Saxena A, Gupta N, Kapoor H, Singh RP (2010) Biological synthesis of silver nanoparticles by using onion (Allium cepa) extract and their antibacterial activity. Digest J Nanomat Biostruc 5:427–432
25. Rodriguez-Sanchez L, Blanco MC, Lopez-Quintela MA (2000) Electrochemical synthesis of silver nanoparticles. J Phys Chem 104:9683–9688
26. Taleb A, Petit C, Pileni MP (1997) Synthesis of highly monodisperse silver nanoparticles from AOT reverse micelles: a way to 2D and 3D self-organization. Chem Mater 9:950–959
27. Ara BN, Samiran M, Saswati B, Rajibul AL, Debabrata M (2009) Biogenic synthesis of Au and Ag nanoparticles using aqueous solutions of Black Tea leaf extracts. Colloids Surf B Biointerfaces 71:113–118
28. El-Daly SA, Alamry KA, Asiri AM, Hussein MA (2012) Spectral characteristics and fluorescence quenching of N, N'-bis(4-pyridyl)-3,4:9,10-perylenebis(dicarboximide) (BPPD). J Lumin 132: 2747–2752
29. Perrin J (1932) Theorie quantique des transferts d'activation entre molecules de meme espece. Cas des solutions fluorescents. Ann Phys 179:283–314
30. Shelli R, Coffer JL (1992) Deactivation of Q-cadmium sulfide photoluminescence through polynucleotide surface binding. J Phys Chem 96:10581–10584
31. Jhonsi MA, Kathiravan A, Renganathan R (2009) Photoinduced interaction between xanthene dyes and colloidal CdS nanoparticles. J Mol Struct 921:279–284